Effect of impurities on magnetic properties of $Y(Co_{5-x}Cu_x)$ and $Y_2(Co_{7-x}Ni_x)$

P. Larson*, I.I. Mazin

Naval Research Laboratory, Center for Computational Materials Science, 4555 Overlook Avenue SW, Washington, DC 20375-5320, USA

Abstract

Doping of the magnetic materials $SmCo_5$ and Sm_2Co_7 with Cu or Ni enhances the magnetic properties by aligning otherwise independent domains. However, this doping with non-magnetic elements also decreases the magnetic moments of the Co atoms, which we have studied using density functional theory (DFT) calculations. Since localized Sm f-orbitals are very difficult to study within DFT calculations, we have studied $Y(Co_{5-x}Cu_x)$, $Y(Co_{5-x}Fe_x)$, and $Y_2(Co_{7-x}Ni_x)$. While the total magnetic moments appear to follow the virtual crystal approximation (VCA) for the Ni and Cu doping, the localized moments on the Co atoms reduce much slower than expected from the VCA before suddenly dropping to zero at a critical concentration. The magnetic moments of $Y(Co_{5-x}Cu_x)$ have been studied as a function of unit cell volume and c/a ratio which show sudden decreases in both the total and localized moments. In contrast, the magnetic moments of $Y(Co_{5-x}Fe_x)$ increase with doping, but the magnetic anisotropy energy decreases, which is not useful technologically.

1. Introduction

Alignment of domains in hard magnetic materials is often facilitated by addition of non-magnetic elements, leaving chemically different products between the grains. Ni- and Cu-doped alloys of $SmCo_5$ and Sm_2Co_7 have been found between the grains of the Ni- and Cu-doped permanent magnet material Sm_2Co_{17} [1]. Both $SmCo_5$ and Sm_2Co_7 are also hard magnetic materials which are technologically important. The addition of the non-magnetic dopants in $SmCo_5$ and Sm_2Co_7 reduce their total magnetic moments. Due to the problems of localized f-electrons in density functional theory (DFT) [2], such as in Sm, we have studied $Y(Co_{5-x}Cu_x)$ and $Y_2(Co_{7-x}Ni_x)$. While the difference in the f-shells of Y and Sm plays an important role in the resulting magnetic anisotropy, the f-electrons participate very little in the bonding and, therefore, the corresponding Y compounds should give useful insights to the energetics of the doping in the Sm–Co systems.

*Corresponding author.

E-mail address: larson@dave.nrl.navy.mil (P. Larson).

We have used supercell calculations with ordered impurities to imitate the random $Y(Co_{5-x}Cu_x)$ and $Y_2(Co_{7-x}Ni_x)$ alloys. We have also performed virtual crystal approximation (VCA) [3] calculations where an ordered compound with a hypothetical element with a non-integer atomic number, such as $Z = 27 + x$ for $Y_2(Co_{7-x}Ni_x)$ or $Z = 27 + 2x$ for $Y(Co_{5-x}Cu_x)$, is substituted for Co. We found that the total magnetic moment is reasonably close to the VCA results. However, this agreement is misleading. While the averaged moment of Co and Cu atoms follows the VCA, the individual Co moments do not. In fact, the Co moments retain their localized character up to some critical dopant concentration where their moments rapidly drop to zero.

A sudden decrease of the magnetic moment is also found by changing the volume of the unit cell. The individual Co magnetic moments in $Y(Co_{5-x}Cu_x)$ show a collapse with respect to unit cell volume, but not with respect to c/a ratio. Unlike the Ni moments in the previous calculation of $Y(Co_{5-x}Ni_x)$ [4,5], the Cu moments in $Y(Co_{5-x}Cu_x)$ do not show a sudden increase or decrease with volume.

2. Method and crystal structure

The crystal structure of YCo_5 is that of $CaCu_5$ (P6/mmm, No. 191). The experimental values of a and c/a used in the calculation for $Y(Co_{5-x}Cu_x)$ are 9.313 a.u. (a.u. = atomic unit or Bohr) and 0.806. The Co sites are separated into two sets of inequivalent atoms, Co(2c) with two-fold multiplicity and Co(3g) with three-fold multiplicity [6]. The crystal structure is shown in Fig. 1. The crystal structure of Y_2Co_7 is that of Er_2Co_7 (R3m, No. 166). The experimental values of a and c/a used in the calculation for $Y_2(Co_{7-x}Ni_x)$ are 9.49 a.u. and 7.229. The simplest unit cell consists of two sets of Y atoms, Y(6c1) and Y(6c2), each having two-fold multiplicity. The Co atoms are separated into five sets of inequivalent atoms: Co(3b), which has single multiplicity; Co(6c1) and Co(6c2), each having two-fold multiplicity; Co(9e), having three-fold multiplicity; and Co(18h), having six-fold multiplicity. The crystal structure is shown in Fig. 2 [6].

Electronic structure calculations of the magnetic moments at fixed lattice constants were performed using the self-consistent linearized muffin-tin orbital method within the atomic sphere approximation (LMTO-ASA) [7]. The von Barth–Hedin exchange correlation potential [8] was used for the local density approximation (LDA). Calculations were performed for 64 **k**-points within the irreducible Brillouin zone. Since the total energies are known to be sensitive to the muffin-tin sphere chosen, the full-potential linearized augmented plane wave (FLAPW) [9] method was used in the calculations involving the volume and/or c/a ratio
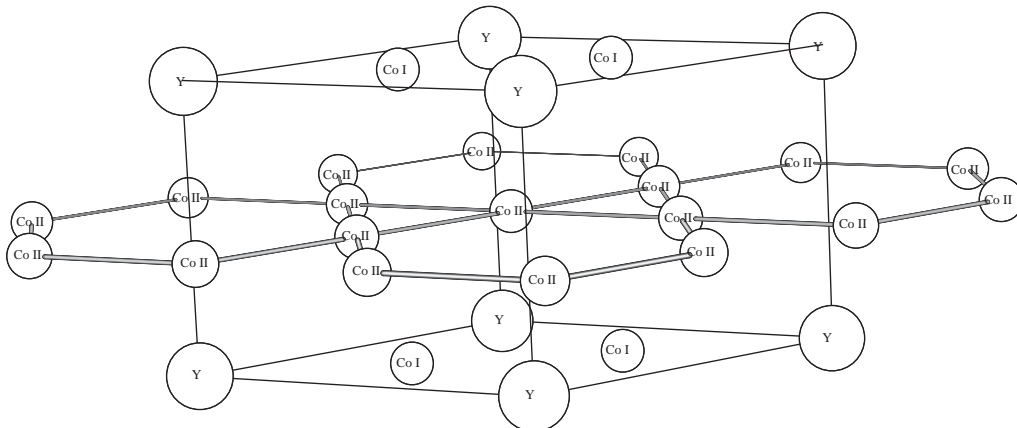

Fig. 1. Crystal structure of YCo_5. While Y forms a triangular lattice and CoI forms a hexagonal lattice in the xy plane, the CoII lattice is a kagome lattice in the xy plane.
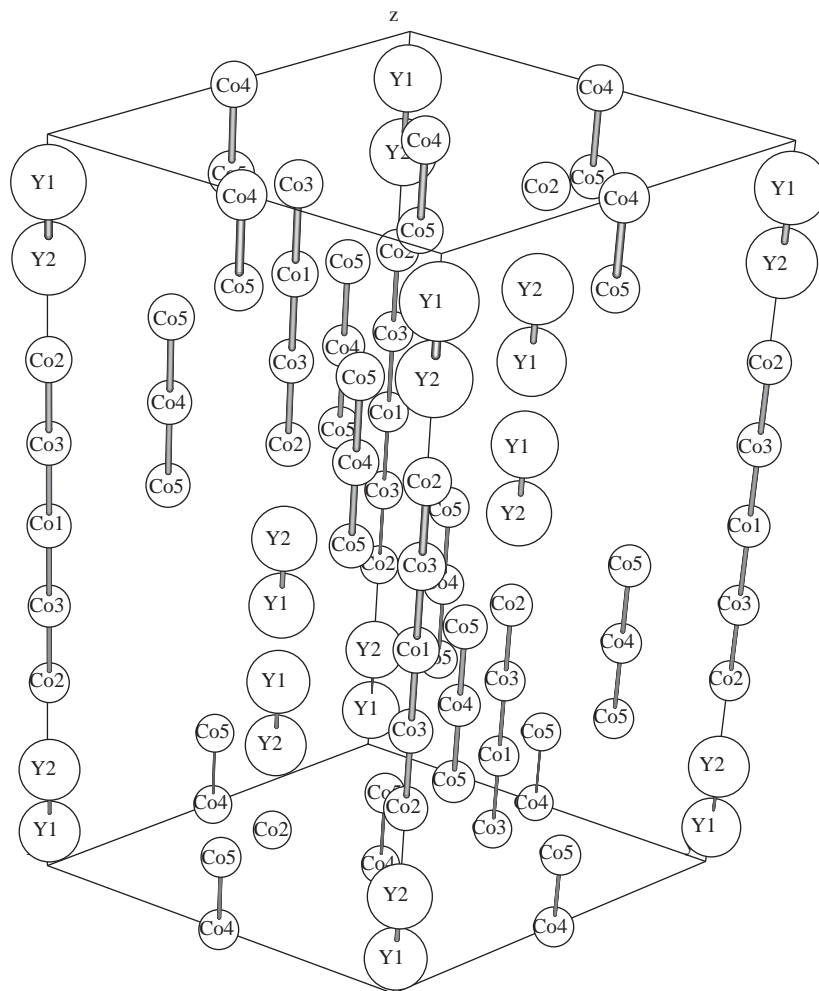
Fig. 2. The crystal structure of Y_2Co_7 is similar to that of YCo_5 with dumbbells forming along the z-axis. Y1–Y2 and Co2–Co3–Co1–Co3–Co2 form chains which have triangular symmetry in the plane. Co5–Co4–Co5 chains have the same symmetry as CoII in $SmCo_5$. The c/a ratio is not shown here to scale.

changes, as well as for the magnetic anisotropy calculations which require high accuracy. The muffin-tin radii were kept at a fixed value in all calculations. The generalized gradient approximation (GGA) of Perdew et al. [10] was used for the correlation and exchange potentials. Calculations were performed using the WIEN97 package [11] for 28 **k**-points within the irreducible Brillouin zone. In these calculations, convergence in energy was within 0.0001 Ry with RKMAX chosen as 8 and GMAX as 10 a.u.$^{-1}$. Scalar relativistic corrections were added for all systems and SO was

incorporated for the FLAPW calculations using a second variational procedure [13]. Local orbitals extensions [12] were included to accurately treat the semicore states as well as to relax any residual linearization errors.

The calculations have been performed for integer x's by placing one or more dopant Cu atoms in the Co sublattices. Unless $x = 2$ or $x = 3$, this leads to a symmetry reduction. An experimentally important question is whether the dopant atoms are distributed homogeneously on one of the two Co sublattices or if one of the two is

preferentially occupied. We have compared the total energies for YCo_4Cu_1, where Cu substitutes Co in the first or in the second sublattice, in order to answer this question.

3. Results

3.1. Doping effects

As mentioned above, the first question to be addressed is whether there is a preferential occupancy of the two inequivalent Co sites by the Cu dopant atoms. We have performed FLAPW calculations for the total energy of YCo_4Cu_1 for the two possible substitutions, and have found that when the Cu atom was on one of the Co1(2c) sites, the energy was 0.13 eV/Cu, or ≈ 1500 K/Cu, lower than when the Cu atom was on one of the Co2(3g) sites. We also find 0.13 eV/Cu for YCo_3Cu_2 with the Cu in the Co1(2c) sites rather than the Co2(3g) sites. This implies preferential filling of the Co1(2c) for low Cu concentrations.

The effects of Cu and Ni doping on the magnetic moments of $SmCo_5$ and YCo_5 have been studied in several experiments [14–20]. It was observed that the total magnetization and the anisotropy field of annealed $Sm(Co_{5-x}Cu_x)$ decrease linearly as a function of Cu concentration, becoming zero around $x = 3$ [14]. Later works found that annealing has a strong effect on the measured magnetic properties [15–17]. This agrees with our finding that there is a preferential occupation with a substantial energy gain, which can be achieved by annealing. The magnetization of Ni-doped YCo_5 has also been found to decrease with doping, vanishing around a Ni concentration of 60% [18,19]. This is in agreement with the above argument that the f-electrons of Sm have little effect on all properties except the magnetic moment on the rare-earth site and magnetic anisotropy, and that one can avoid the difficulties of treating the strongly correlated Sm f-levels by using doped YCo_5 to understand the effects of doping on the magnetic moments.

The effects of doping on the magnetic moment are often nonlinear. For instance, the observed
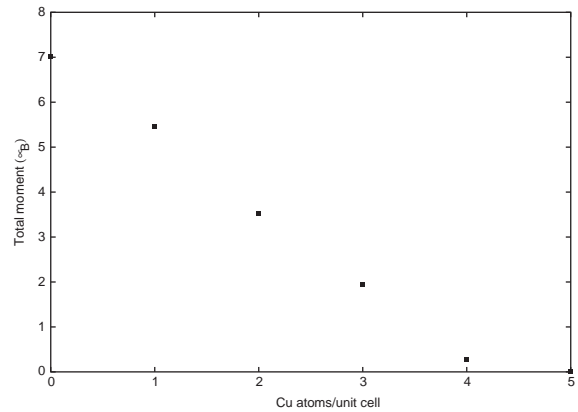

Fig. 3. Total moment of $YCo_{5-x}Cu_x$ as a function of doping.

magnetic moment of $Y(Co_{5-x}Ni_x)$ shows a sudden drop near $x = 3$ [21]. In a recent LMTO-ASA calculation, Yamada et al. [5] used the VCA [3] for $Y(Co_{5-x}Ni_x)$, finding a modest drop in the magnetic moments around $x = 2.5$ in an otherwise fairly linear regime. The difference between the sharp jump seen experimentally and the modest drop in the calculation was attributed to the effect of the local environment of the Co atoms within the alloy [5].

Our calculations of $Y(Co_{5-x}Cu_x)$ show that the total magnetic moment/unit cell decreases fairly linearly with Cu doping (Fig. 3), similar to the previous results found with Ni doping [5]. This suggests that the effect of Cu doping on magnetism is mostly due to the electronic doping, not simply to the nonmagnetic nature of Cu. However, if that were the case, one would not only expect total magnetic moment reduction but also somewhat delocalized Co moments. This would follow the VCA approximation [3], employed by Yamada et al. [5]. However, a closer inspection of our results reveals that the magnetic moment on Co is fairly local and little affected by the Cu doping until $x \sim 2.5$ where the moment rapidly falls to a small value before gradually decaying to zero (Fig. 4). We conclude that Co in doped YCo_5 can occur either in a high- or low-spin state, depending on the local environment. Presumably, in disordered alloys both spin states are present, the low-spin state in the locally Cu-rich regions, and the high-spin state elsewhere. The crossover concentration

of $x \sim 2.5$–3 is characterized by a change from mostly high-spin Co to mostly low-spin Co. This crossover concentration is the same as has been
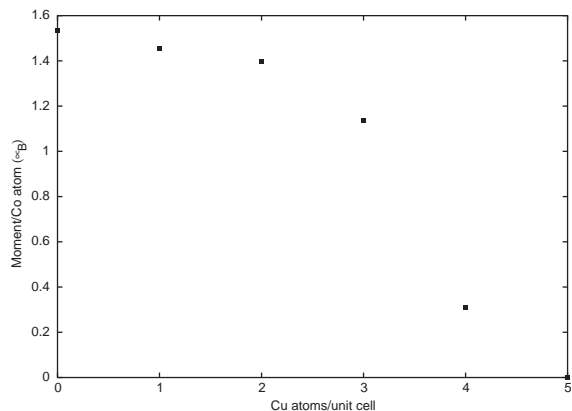

Fig. 4. Averaged Co moment of $YCo_{5-x}Cu_x$ as a function of doping.

observed experimentally for the decrease of the total magnetization [18,19].

Physically, this behavior can be understood from a study of the density of states (DOS) plots (Fig. 5). The main effect of Cu doping (panels b–e) is the appearence of an additional d-band (predominantly of Cu character) 3–4 eV below the Fermi level. However, as long as the DOS at the Fermi level remains sufficiently large, the nonmagnetic state is unstable, and a ferromagnetic states forms where the exchange splitting is large enough to make the peak at the Fermi level fully occupied (further splitting gains little exchange energy and costs a lot of kinetic energy). Therefore, the magnetic moment *per Co* changes relatively little, to the extent of admixture of the Cu states into the predominantly Co-d upper peak. At a sufficiently large doping (Fig. 5f) the upper peak is removed from the Fermi level leaving the
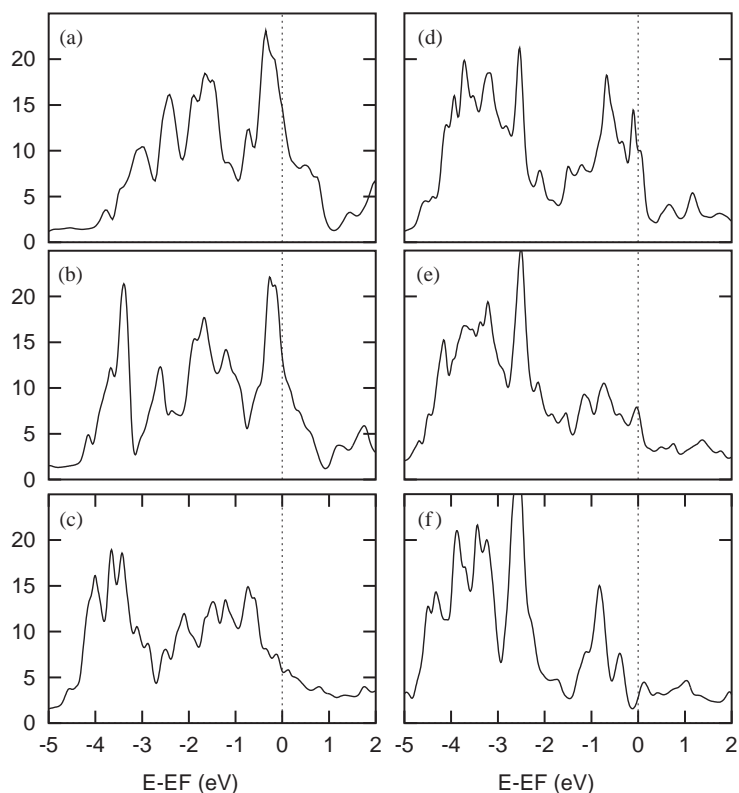

Fig. 5. Density of states in *paramagnetic* $YCo_{5-x}Cu_x$ for (from a to f) $x = 0, 1, 2, 3, 3.5$ and 4. To simplify the comparison, the curves were smoothed. Also, for $x = 3$ and 3.5 two different unit cells with the same nominal composition were used and these results were averaged.
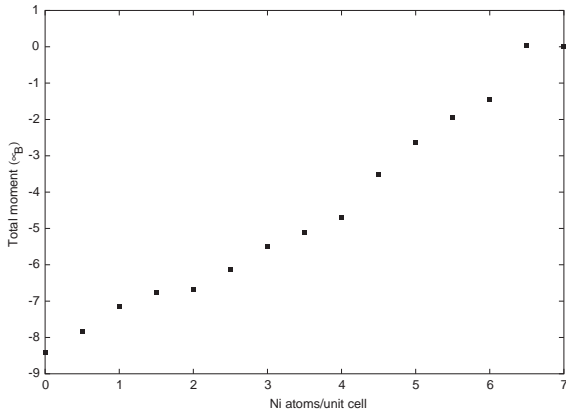
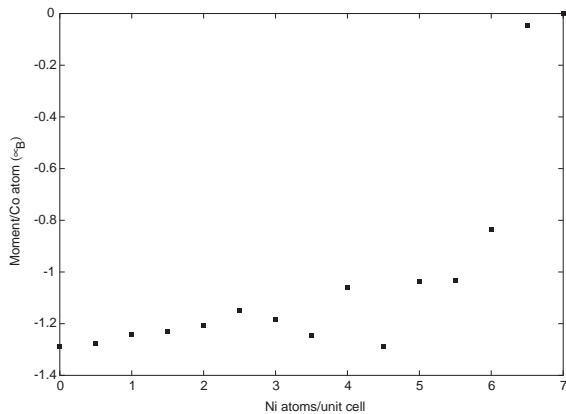Fig. 6. Total moment of $Y_2Co_{7-x}Ni_x$ as a function of doping.

Fig. 7. Averaged Co moment of $Y_2Co_{7-x}Ni_x$ as a function of doping.

Cu-d levels, which are already in the paramagnetic state. This paramagnetic state then becomes stable.

We found a similar behavior in the total and Co magnetic moments as in $Y_2(Co_{7-x}Ni_x)$, as seen in Figs. 6 and 7. Note that within the same supercell there may be more than one possible configurations for a specific x, therefore, for some x the moment shown in the plot is averaged over the different configurations. As in $Y(Co_{5-x}Cu_x)$, the total moment (in absolute value) decreases linearly to 0 at $x = 7$ (Fig. 6). The moments on the inequivalent Co sites differ slightly due to their different local environments. However, the aver-

age Co moment decreases slightly up to $x = 6$, and then rapidly goes to the low-spin state (Fig. 7). The fluctuations seen for $x = 4.0$, 4.5, and 5.0 are most likely due to the limited number of possible orderings of the Co and Cu atoms within this particular supercell. The Co moments for these configurations allowed by symmetry have a strong dependence on the local environment of the Co atom. This variation should decrease by averaging over more configurations using larger supercells.

3.2. Shape and volume effects

A similar collapse of the magnetic moments occurs under pressure (hydrostatic or uniaxial). In two previous works, the effect of hydrostatic pressure (with the c/a ratio fixed) on the total and Co magnetic moments has been studied in several $Y(Co_{5-x}Ni_x)$ systems [4,5]. It was found that for doped systems the magnetic moment collapse occurs at lower pressures (Fig. 8 and results for Ni doping in Ref. [4]). Experimental measurements of the moments in these alloys at ambient pressure show a sudden drop in the moments between $x = 2$ and 3 [18,19]. The previous calculations [4,5] found that, regardless of doping, the moment experiences a sudden decrease as pressure is increased. The measured moment depended on whether the moment was large or small at the equilibrium volume.

We have carried out similar calculations for YCo_5, YCo_3Cu_2, and YCu_5. As seen before for Ni
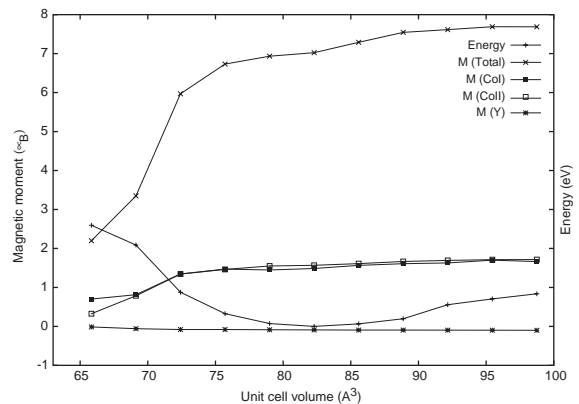

Fig. 8. Total energies and Y and Co moments of YCo_5 as a function of volume.

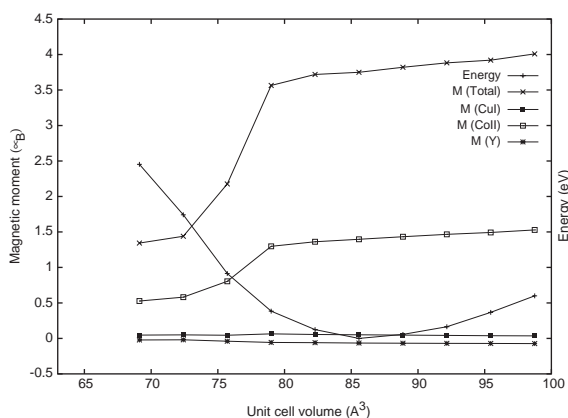Fig. 9. Total energies and Y and Co moments of YCo_3Cu_2 as a function of volume.

Fig. 10. Total energies and Y and Co moments of YCo_5 as a function of c/a ratio.

doping [4,5], the first two systems studied have a sudden drop in the moment as a function of pressure (Figs. 8 and 9). The Co moments in these systems collapse to a low-spin state under pressure. There are two significant differences from the previously studied Ni case. First, the Cu moment remains almost zero for all volumes in all of the systems studied, not showing a sudden decrease as had been seen in the Co or Ni moments. This means that the Cu moment does not contribute to the total moment of the $Y(Co_{5-x}Cu_x)$ alloys in the same way that the Ni moments contributed to the $Y(Co_{5-x}Ni_x)$ alloys. Second, the Co moment remains large at the equilibrium configuration for YCo_3Cu_2. This sudden transition from a high- to a low-spin state can be used to explain the differences between Cu and Ni doping in YCo_5. For Ni doping, the size of the unit cell decreases with increasing Ni concentration. For some doping levels, the equilibrium volume lies below the high-/low-spin transition. Therefore, the reduction of the moments is not due just to fewer Co atoms in the unit cell but to crossing over this transition, leading to a jump in the magnetic moments as a function of doping [4]. For Cu doping, the size of the unit cell increases with doping (Fig. 9), so that the reduction of the magnetic moments as a function of doping is due only to having fewer Co atoms in the unit cell. Recent experimental studies of the magnetic properties of $Y(Co_{5-x}Cu_x)$ alloys do not find a decrease of the magnetic
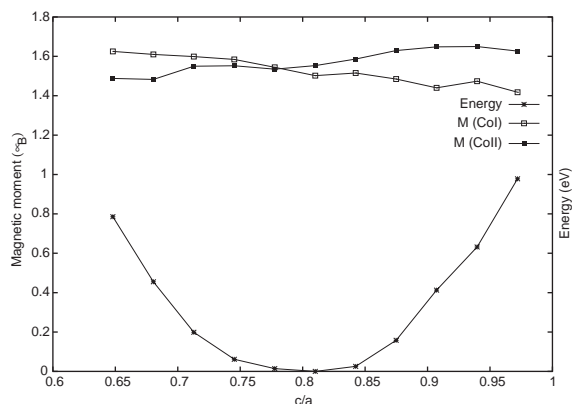
moment as a function of doping as had been found in their Ni counterparts [20]. In fact, while the cell volume is found to decrease experimentally with Ni doping, the cell volume is seen to increase experimentally with Cu doping [19,20].

Given such a strong effect of hydrostatic pressure on the Co moment, it is important to study the effects of a uniaxial compression as well. Our results for YCo_5 (Fig. 10) show that the variation of the moments with the c/a ratio is relatively small, less than 10% of their equilibrium value for c/a ratios varying from 0.625 to 0.975. The Co(2c) moment is larger at smaller c/a ratios but decreases at larger c/a ratios. The Co(3g) moment exhibits exactly the opposite behavior, smaller at small c/a ratios and larger at large c/a ratios. The sum of the Co moments remains constant, the total moment shows almost no variation as a function of c/a ratio.

3.3. Magnetic anisotropy

Since doping with Cu or Ni reduces the magnetization, the magnetic anisotropy energy, naturally, decreases as well. In the case of Fe doping, which actually increases the magnetization, the effect on the magnetic anisotropy energy (MAE) is hardly obvious. We have studied the MAE and moments of $Y(Co_{5-x}Fe_x)$ (Fig. 11). While the total moment is increased by Fe doping, the MAE is not similarly increased. In fact, the
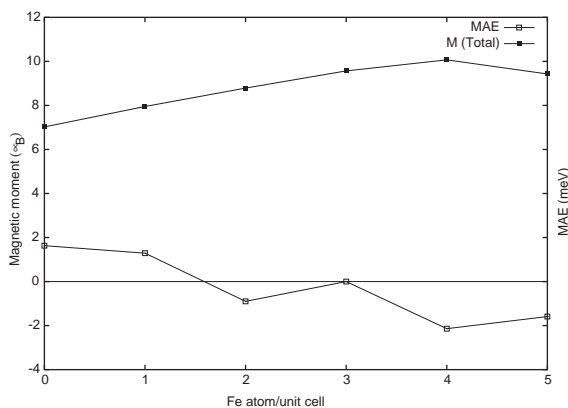
Fig. 11. Total moments and MAE of $Y_2Co_{7-x}Fe_x$.

MAE reduces with Fe concentration and changes sign with large Fe concentration, which is not the direction preferable for applications with hard magnets in devices [1]. While one could suspect that Fe doping would improve the magnetic properties, it appears that large dopings adversely affect the MAE.

4. Conclusions

Our calculations of the magnetic moments in $Y(Co_{5-x}Cu_x)$ and $Y_2(Co_{7-x}Ni_x)$ show that the moments of these alloys remain localized on the Co moments with an unexpected dependence on concentration. While the total moments follow the VCA, the individual Co moments decrease slowly with a sudden drop to zero at a critical concentration. The total moments also show a sudden decrease as a function of volume at a fixed concentration. While the minimum energy configuration for YCo_3Ni_2 lies at a volume where the Co moment is nearly zero, the minimum energy configuration for YCo_3Cu_2 remains fairly large, both results having been seen experimentally. Rather than the gradual change of the magnetic moments in YCo_5 and Y_2Co_7 as seen in the total moments and predicted by the VCA, the localized Co moments show abrupt changes. Doping with Fe, on the contrary, increases the total magnetic moment, but appears to adversely affect the magnetic anisotropy energy.

References

[1] J.C. Blanco, X.C. Kou, R. Grossinger, E. Estevez-Rams, J. Fidler, and B.M. Ma in: F.P. Missell, et al., (Eds.), Proceedings of the 14th International Workshop on Rare Earth Magnets and their Applications, 1996, p. 707.

[2] M.S.S. Brooks, L. Nordstrom, B. Johansson, J. Phys.: Condens. Matter 3 (1991) 3393.

[3] L. Nordheim, Ann. Phys. 9 (1931) 607.

[4] I. Kitagawa, K. Terao, M. Aoki, H. Yamada, J. Phys.: Condens. Matter 9 (1997) 231.

[5] H. Yamada, K. Terao, F. Ishikawa, M. Yamaguchi, H. Mitamura, T. Goto, J. Phys.: Condens. Matter 11 (1999) 483.

[6] R.W.G. Wyckoff, Crystal Structures, Vol. 2, Krieger, Melbourne, FL, 1986.

[7] R. Tank, O. Jepsen, A. Burkhardt, O.K. Anderson, Tight-binding LMTO Version 4.7, Max-Planck-Institut fur Festkoperforschung, 1994 (unpublished).

[8] U. von Barth, L. Hedin, J. Phys. C 5 (1972) 1629.

[9] D. Singh, Planewaves, Pseudopotentials, and the LAPW Method, Kluwer Academic, Boston, 1994.

[10] J.P. Perdew, K. Burke, M. Ernzerhof, Phys. Rev. Lett. 77 (1996) 3865.

[11] P. Blaha, K. Schwarz, and J. Luitz, WIEN97, A Full Potential Linearized Augmented Plane Wave Package for Calculating Crystal Properties, Karlheinz Scwarz, Technical Universitat Wien, Austria, 1999, ISBN 3-9501031-0-4.

[12] D. Singh, Phys. Rev. B 43 (1991) 6388.

[13] D.D. Koelling, B. Harmon, J. Phys. C 10 (1997) 3107; P. Novak, unpublished.

[14] E. Lectard, C.H. Ailbert, R. Ballou, J. Appl. Phys. 75 (1994) 6277.

[15] J.C. Tellez-Blanco, R. Grossiner, R. Sato Turtelli, J. Alloys Compounds 281 (1999) 1.

[16] J.C. Tellez-Blanco, R. Sato Turtelli, R. Grossinger, J. Appl. Phys. 86 (1999) 5157.

[17] A-ru Yan, Wen-yong Zhang, Hong-wei Zhang, Bao-gen Shen, J. Appl. Phys. 88 (2001) 2787.

[18] Y.C. Chuang, C.H. Wu, Y. Chang, J. Less-Common Met. 84 (1982) 201.

[19] V. Crisan, V. Popescu, A. Vernes, D. Andreica, I. Burda, S. Cristea, J. Alloys Compounds 223 (1995) 147.

[20] J.C. Tellez-Blanco, R. Grossinger, R. Sato Turtelli, E. Estevez-Rams, IEEE Trans. Magn. 36 (2000) 3333.

[21] M.I. Bartashevich, T. Goto, A. Korolyov, A.S. Ermolenko, J. Magn. Magn. Mater. 163 (1996) 199.